Rear point contact structures for performance enhancement of semi-transparent ultrathin Cu(In,Ga)Se_2 solar cells

Guanchao Yin[1, 2, *], Ming Song[1, 3], Martina Schmid[1, 4]

[1]Nanooptical Concepts for PV, Helmholtz-Zentrum Berlin für Materialien und Energie, Hahn-Meitner Platz 1, 14109 Berlin, Germany

[2]School of Materials Science and Engineering, Wuhan University of Technology, Luoshi Road 122, 430070 Wuhan, China

[3]Department of Physics, Freie Universität Berlin, Arnimallee 14, 14195 Berlin, Germany

[4]Department of Physics, Universität Duisburg-Essen & CENIDE, Lotharstraße 1, 47057 Duisburg, Germany

[*]Corresponding author: guanchao.yin@whut.edu.cn (Guanchao Yin)

ABSTRACT: Semi-transparent ultrathin Cu(In,Ga)Se_2 (CIGSe) solar cells offer many promising applications but their efficiencies are still limited. In this work, SiO_2 point contact structures were prepared using nanosphere lithography on Sn:In_2O_3 (ITO) substrate and ultrathin CIGSe solar cells were fabricated on top. It was discovered that the SiO_2 point contact structure at the CIGSe/ITO interface behaves significantly different from at the CIGSe/Mo interface and does not improve the rear interface reflectivity or short-circuit current density. However, the SiO_2 point contact structure brings pronounced electrical benefits, arising from the joint effect of reduced back recombination and induced field effect by internal charges. Semi-transparent ultrathin CIGSe solar cells with an absorber thickness of 380 nm exhibited a significant increase in open circuit voltage of 26 mV and fill factor of 9.4% (absolute). Consequently, the efficiency is improved by 23% (from absolute 6.8% to 8.4%).

KEYWORDS: point contact, back contact passivation, ultrathin CIGSe solar cells, transparent back contact, nanosphere lithography

1 Introduction

$CuIn_{1-x}Ga_xSe_2$ (CIGSe) solar cells have been attracting extensive attention in the photovoltaic market. Besides high record efficiencies [1,2], CIGSe solar cells are holding unique features of a remarkably short energy payback time, minimal consumption of high purity materials and great tolerance to the variations of working conditions, offering them a great potential to compete with the dominant crystalline Si solar cells on the market [3]. However, mass production is likely to impact the supply of element In and Ga and thus reduces the competitiveness of CIGSe solar cells [4,5]. Therefore, an ultrathin absorber (< 500 nm) can significantly reduce the consumption of high purity materials and related cost. Further， it relaxes the requirements for CIGSe absorber qualities since the diffusion lengths of minority carriers are much reduced [6]. Conventionally, Mo is used as back electrode materials. Apart from its conductivity and good adhesion with CIGSe, excellent thermal stability for CIGSe deposition and the formation of an ohmic contact with CIGSe absorbers make Mo a unique option as back contact for CIGSe solar cells. However, Mo has intrinsic opaque property and exhibits poor interface reflectivity at the rear CIGSe/Mo interface, limiting the exploration of advantages for ultrathin CIGSe solar cells. Alternatively, CIGSe solar cells can be deposited on transparent conductive oxides (TCOs) such as $F:SnO_2$ (FTO), Al:ZnO (AZO), $Sn:In_2O_3$ (ITO) [7,8]. It has been reported that ultrathin CIGSe cells (with a sub-500 nm absorber thickness) on TCO back contact are able to achieve a comparable absorption to their thick counterparts via light trapping structures [9]. Additionally, the TCO back contacts permit the application of CIGSe solar cells in multi-junction configuration as top cell [10,11], bifacial solar cell [12], solar window and backwall configuration (back illumination) [13,14].

It has been extensively demonstrated that rear point-contact structures are able to passivate the CIGSe/Mo interface and improve the CIGSe/Mo interface reflectivity for optoelectronic enhancement of ultrathin CIGSe solar cells [15–19]. However, the work so far is merely on Mo-based ultrathin CIGSe solar cells. Considering the promising application of TCO-based ultrathin CIGSe solar cells, it will be meaningful to investigate whether the point contact structures are working efficiently for CIGSe solar cells on TCO.

In this work, we prepared periodically SiO_2 point contact structures on ITO back contact using nanosphere lithography method. It is experimentally discovered that the point contact structures are capable of passivating the rear CIGSe/ITO interface for performance enhancement of ultrathin CIGSe solar cells. Semi-transparent ultrathin CIGSe solar cells with a 380 nm thick absorber show an improvement of 26 mV in open-circuit voltage (V_{oc}) and of 9.4% in fill factor (FF), respectively. As a result, the SiO_2 point contact structures give rise to a relative efficiency enhancement by 23%.

2 Experiments and characterizations

2.1) Point contact structure preparation

We employ the method of nanosphere lithography [20,21] to fabricate point contact structures. Figure 1 depicts the flow of the fabrication process. Commercial polystyrene (PS) latex solution is first mixed with ethanol in 1:1 volume and dipped at air/water interface by using a curved glass pipette. A closely packed PS spheres form a monolayer on the water surface. ITO substrates are carefully submerged in the water and the PS monolayer is then transferred to ITO surface by sucking out water. Subsequently, the PS spheres are etched from original 900 nm down to 600 nm in diameter by O_2 plasma at a bias pressure of 0.2 mbar for 12 minutes. Subsequently, the reduced PS spheres can serve as a mask for direct thermal evaporation of a 50 nm thick SiO_2 layer. Finally, the ITO substrates are placed in toluene to lift off the reduced PS nanospheres and SiO_2 point contact structures then remain on the ITO substrates.

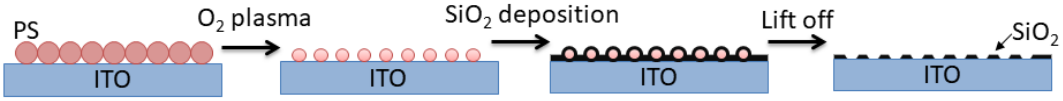

Figure 1 Schematic illustration of preparation flow of SiO_2 point contact structures on ITO using nanosphere lithography

2.2) Solar cell preparation and characterization

ITO substrates are sputtered with a thickness of 200 nm and a sheet resistance <10 ohm/sq. For solar cell completion, CIGSe absorbers are co-evaporated on ITO substrate via the so-called 3-stage process [22]. To avoid deteriorating ITO properties, a low substrate temperature of 450 °C is employed. Afterwards, a 50 nm CdS thin film

is deposited on top of CIGSe via chemical bath deposition for the formation of pn junction, which is followed by a sputtered 130 nm i-ZnO and a 240 nm ZnO:Al layer. For performance measurements, metal front contact grids (Ni/Al) are evaporated through a shadow mask and solar cells are mechanically divided and the area of a single cell is 0.5 cm^2.

For the observation of morphology of point contact structures and solar cells, scanning electron microscopy (SEM) is employed using the signal of back scattering electrons. Wavelength-dispersive X-ray fluorescence analysis (XRF) is used to accurately measure CIGSe absorber compositions and thicknesses. An overall Ga/(Ga+In) ratio of 0.38 as well as a Cu/(Ga+In) ratio of 0.88 is obtained. The absorbers have a thickness of 380 nm. For electrical characterization, the current density−voltage (*JV*) curves are recorded under standard AM 1.5 illumination condition by a sun simulator and the external quantum efficiency (EQE) is measured from wavelength 300 nm to 1200 nm.

3 Results and discussion

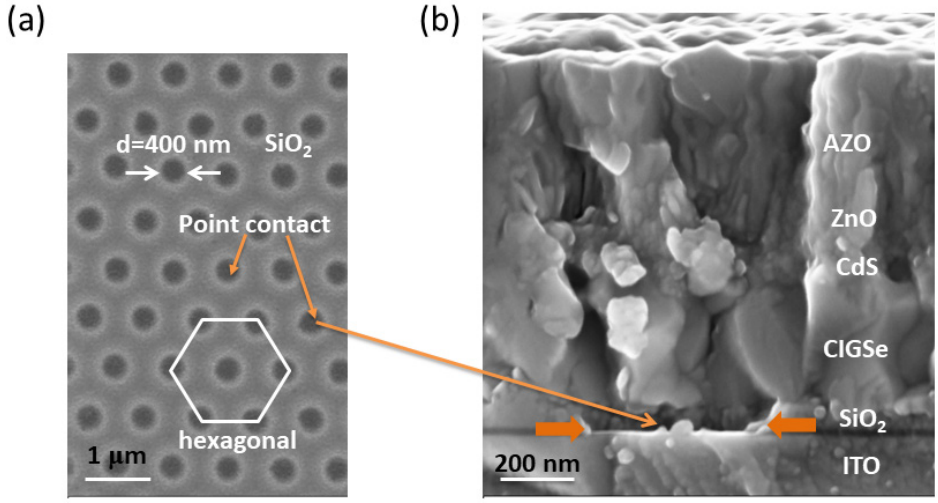

Figure 2 (a) SEM image of SiO_2 point contact structures on ITO substrate and (b) cross section of a complete CIGSe solar cell on the SiO_2 point contact structure

Figure 2(a) shows a representative SEM image of the SiO_2 point contact structure on ITO substrate fabricated using nanosphere lithography. The point contacts (holes in the image), corresponding to the remaining surface of ITO, take the location of the removed PS spheres and follow their hexagonal periodicity. The diameter of a single point

contact is approximately 400 nm, which indicates that as high as 82% area of the substrate is covered by the insulating SiO_2 layer, leaving only 18% of ITO surface as collection channel for holes. An interesting point here is that the diameter of a single point contact (400 nm) is less than a reduced PS sphere mask (600 nm). This phenomenon is arising from our specific preparation setup: the SiO_2 thermal evaporation source is at an oblique angle rather than perpendicular below the sample holder, indicating that the evaporated SiO_2 material can be deposited under the vertical shadow of the PS spheres. Via the rotation of the substrate holder, the reduced PS spheres can thus shadow a smaller area than their geometrical cross sections. It should be stressed here that nanosphere lithography is a promising technology for point contact fabrication. The technology does not require complicated or expensive equipments and the area can be easily scaled to industrial module size [20,23,24]. Additionally, this technology is applicable for a broad range of sizes of PS spheres from micrometer to nanometer, which offers great flexibility to tune the size and distance of neighboring point contacts with the assistance of O_2 plasma etching. This implies that nanosphere lithography can be potentially a universal method to prepare point contacts for various solar cells and other optoelectronic devices.

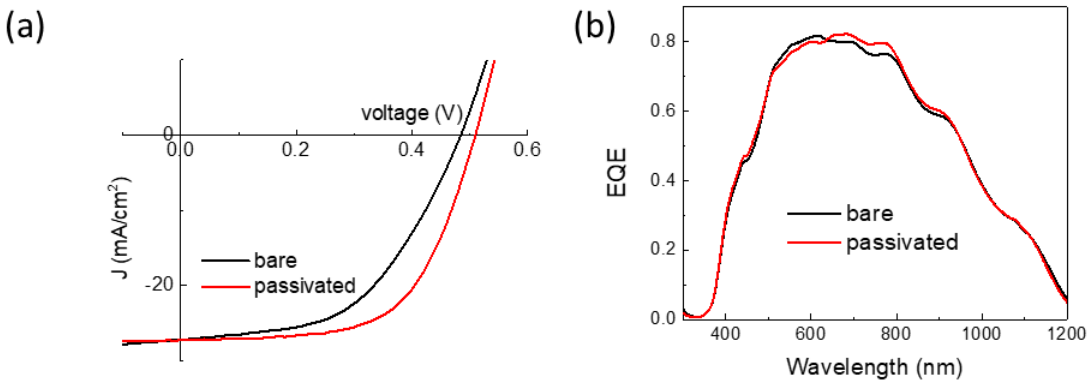

(c)

	V_{oc} (mV)	J_{sc} (mA/cm²)	FF (%)	Eff. (%)
bare	484±5.3	27.2±0.4	51.3±0.5	6.8±0.1
passivated	510±8.4	27.2±0.5	60.7±1.5	8.4±0.6

Figure 3 (a) *JV* curves, (b) EQE and (c) *JV* parameters compared between bare and passivated ultrathin CIGSe solar cells (averaged from 6 samples)

To investigate the influence of point contact structures on the optoelectronic properties of the CIGSe devices, ultrathin CIGSe solar cells with an absorber thickness of 380 nm were fabricated on top. Figure 2(b) shows the cross section of a complete solar cell, where the point contact structures can be observed at the rear interface of CIGSe/ITO and CIGSe absorber grains are closely stacked on top. Figure 3(a) compares the *JV* curves of bare and passivated ultrathin CIGSe solar cells on ITO and the corresponding parameters are listed in Figure 3(c) (averaged from 6 samples). After passivation, both open-circuited voltage (V_{oc}) and fill factor (*FF*) achieve significant enhancement, from 484 to 510 mV and 51.3% to 60.7%, respectively. Short-circuit current density (J_{sc}) remains unchanged. Consequently, the SiO_2 point contact nanostructures overall contribute to a relative efficiency improvement by 23% (from 6.8% to 8.4%).

In our previous study on Mo substrate, the SiO_2 point contact structure is also able to bring obvious J_{sc} enhancement [18], which is however not observed in the case on ITO substrate. EQE curves in Figure 3(b) confirm this: only slight modulation in the spectrum with a drop in the wavelength range of 500-650 nm and an increase in the range of 650-800 nm. As a result, no J_{sc} gain is obtained. Two reasons are assumed to be responsible for this phenomenon: firstly, the effective doping of absorbers for our ultrathin CIGSe solar cells on ITO is only in the order of 10^{15} cm^{-3} (obtained from capacitance-voltage measurement, not shown here), which is one order of magnitude lower than the corresponding value on Mo. This indicates that the space charge region is wide enough, overlaps with the back contact and thereby carrier collection is already optimum in the short-circuit state. Additionally, J_{sc} increase for ultrathin CIGSe solar cells with dielectric point contact structures on Mo substrate is mainly stemming from the absorption enhancement due to improved CIGSe/Mo interface reflectivity [15–18]. However, ITO exhibits different optical properties from Mo, and inserting a SiO_2 layer cannot improve the interface reflectivity of CIGSe/ITO. Since the SiO_2 point contact structures cover an area as high as 82% and are too thin (50 nm thick) to excite nano-optical effects [25], we assumed a planar SiO_2 layer at the rear interface and simulated absorption of the CIGSe layer (Abs_{CIGSe}) of CIGSe cells on (a) ITO and (b) Mo using transfer matrix method in Figure 4, respectively. The thicknesses of each layer were

chosen according to the experimental samples. Optical constants of each layer are from Ref. [26,27] and may pose certain differences from experimental samples, interface roughness is also not considered. It can be observed from Figure 4(a) that a 50 nm thick SiO_2 layer only causes slight modulation of Fabry–Pérot interferences on ITO substrate, which follows the changing trend of experimental EQE data in Figure 3(b). Noticeably, solar cells on Mo (Figure 4(b)) exhibit pronounced and broadband absorption enhancement in the long wavelength region after introducing the thin SiO_2 layer, which poses a sharp contrast to the case on ITO.

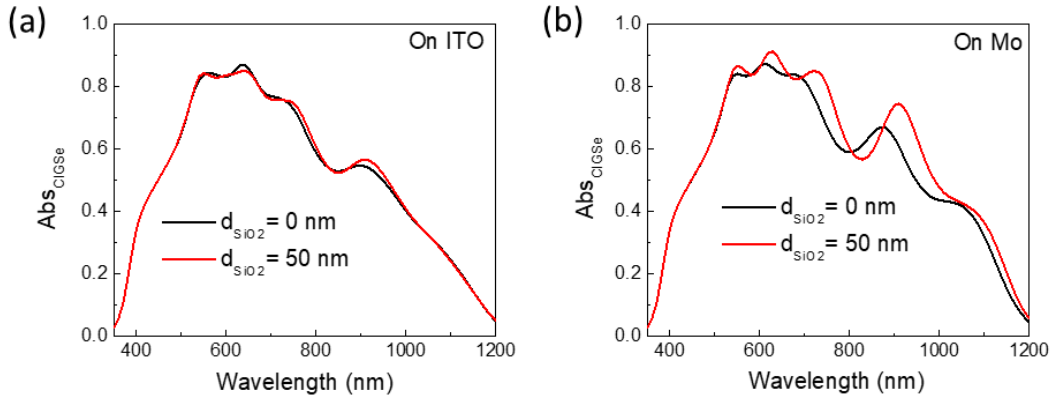

Figure 4 Effects of a SiO_2 layer on absorption in CIGSe (Abs_{CIGSe}) on (a) ITO and (b) Mo substrate

It was widely demonstrated for ultrathin CIGSe solar cells on Mo that a dielectric point contact structure is capable of enhancing cell performance by interface defect passivation and an internal charge-induced field at the rear interface [17,28,29]. However, CIGSe solar cells on ITO typically have a potential barrier and form a Schottky contact because of the mismatch of work function between CIGSe and ITO [13,30], which is different from the cells on Mo with an Ohmic contact. To verify that the point contact structures are able to improve the performance of solar cells with a Schottky back barrier and that the experimental enhancement in electrical properties is arising from the SiO_2 point contact structure, we employ SCAPS [31] for theoretical study. The CIGSe absorber parameters were set according to experimental samples with a thickness of 380 nm, an effective doping of $4*10^{15}$ cm^{-3}, a lifetime of 5 ns and a bandgap of 1.2 eV, other parameters can be found in the supporting information. Due to the general complexity in electrical properties of CIGSe solar cells, the simulation

results here seek for simply explaining the experimental phenomenon rather than to produce exact value match. Figure 5 plots the V_{oc} , J_{sc} and FF variations as a function of back recombination rate and back barrier potential. The recombination rate is varied in the range of 10^2 to 10^6 cm/s since most reported values are in this range [15,17,32]. A back barrier potential ≤ 0.2 eV is typically assumed to be an Ohmic contact [33,34] and a value larger than 0.5 eV will lead to a very poor performance and does not reflect experimental results well, 0.2-0.5 eV was therefore set as the investigated range for back barrier potential. A bandgap diagram of CIGSe/ITO interface is shown in Figure 5(a). In Figure 5(b) it can be seen that as the back barrier potential is rising, V_{oc} is deteriorating for a fixed recombination rate. This is due to the back barrier potential blocking the collection of holes. Experimentally, a back barrier potential ≥ 0.3 eV is expected for our solar cells on ITO [9], V_{oc} is thus poor (< 0.6 eV) and much lower than the corresponding value on Mo (not shown here). Additionally, V_{oc} shows a general increasing trend as the recombination rate is reduced at a fixed back barrier potential. This improvement reflects our experimental observation above as well as other published results for the case on Mo with an Ohmic back contact when the point contact structures are introduced.

Figure 5(c) shows that the J_{sc} value is relatively stable in the broad range of recombination rate ≤ 10^5 cm/s and barrier potential ≤ 0.4 eV. Since the CIGSe thickness is only 380 nm and the entire absorber is therefore within the space charge region, the collection of photogenerated carriers can be guaranteed and thereby J_{sc} is less dependent on recombination rate and barrier potential. This further implies our experimental results where J_{sc} is stable after integrating the point contact passivation structure.

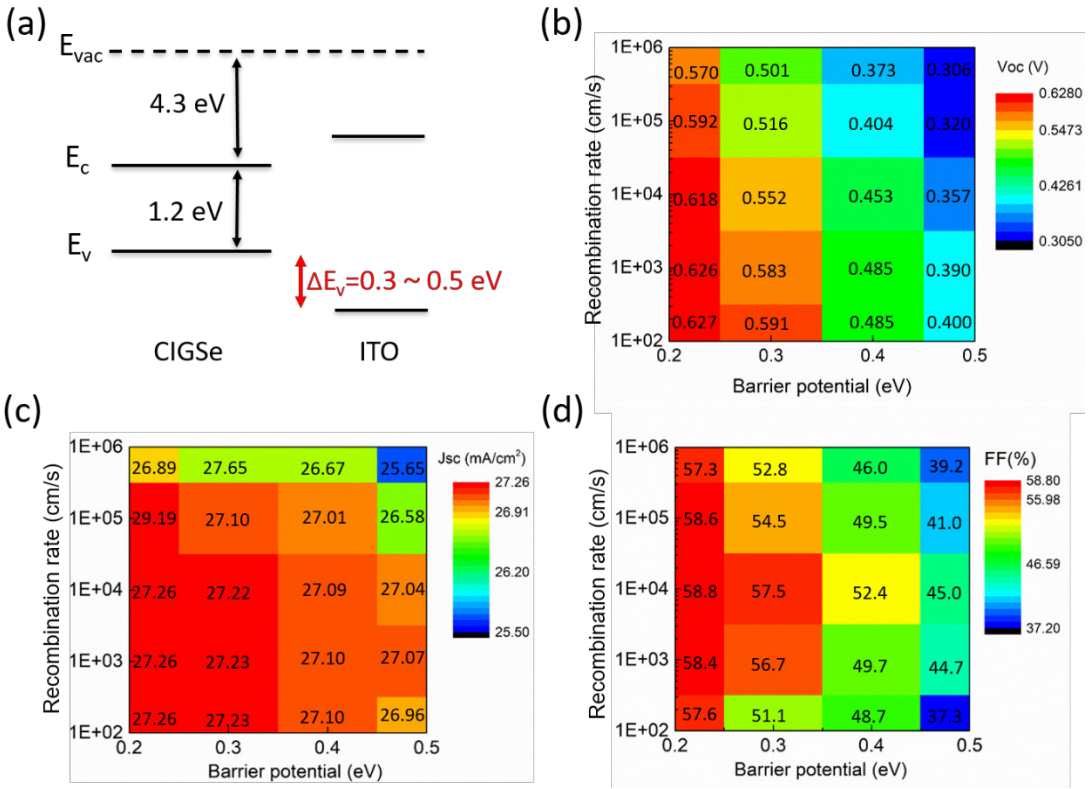

Figure 5 (a) Sketch of bandgap diagram at CIGSe/ITO rear interface, (b) V_{oc}, (c) J_{sc} and (d) *FF* variation as a function of rear recombination rate and back barrier potential

Furthermore, Figure 5(d) depicts that the *FF* reaches the maximum value when the recombination rate is in the order of 10^4 cm/s rather than improving further as the recombination rate becomes smaller. This implies that a reduction of recombination rate may be positive to avoid photo current losses but it is negative in terms of majority carrier (hole) flow. This is why *FF* increases first and then reduces for cells with a Schottky contact, which indicates that further reducing point area (a lower recombination rate) is possibly harmful to *FF* for cells on ITO, which is a sharp difference from solar cells on Mo with an Ohmic back contact.

Besides reduced recombination rate, it was proved that the point contact structures could contain negative internal charges and form a potential for repelling the electron flow towards the back contact [35,36], which benefits electrical properties of solar cells as well. Considering the significant improvement of *FF* (9.4% absolute) in our experiment, it is quite likely that the *FF* improvement after integrating the SiO_2 point contact structure is the joint result of reduced interface recombination rate and field effect of internal charges.

4 Conclusion and outlook

In this work, we investigated the optoelectronic effects of SiO_2 point contact structures on semi-transparent ultrathin CIGSe solar cells. Compared to the case on Mo [18], the SiO_2 point contact structures at the rear interface are not able to improve the interface reflectivity or J_{sc} for ultrathin CIGSe solar cells on ITO. However, the point contact structures give rise to a V_{oc} increase of 26 mV and a *FF* increase of 9.4% absolute。 Thanks to the improvement in electrical properties, ultrathin CIGSe solar cells with a 380 nm thick absorber exhibit an absolute efficiency enhancement of 1.6% (23% relative) after integrating the SiO_2 point contact structures. As the simulations indicated, the reduced rear interface recombination from the point contact structure contributes to the improvement of electrical benefits of ultrathin CIGSe solar cells on ITO with a back barrier.

To further explore the advantages of semi-transparent ultrathin CIGSe solar cells, the next steps are to a) further optimize the geometry and internal charge situation of point contact structures for a greater passivation effect and b) combine point contact structures with hole transporting layers for simultaneously solving the issues of back recombination and non-Ohmic back contact.

ACKNOWLEDGEMENTS

The authors would like to thank C. Kelch, M. Kirsch and J. Albert for technical support, R. Klenk for discussions. The authors acknowledge the funding from the Helmholtz-Association for Young Investigator groups within the Initiative and Networking fund (VH-NG-928). G. Yin acknowledges the funding from National Natural Science Foundation of China (NSFC, 51802240) and M. Song the funding from China Scholarship Council.

References

[1] P. Jackson, R. Wuerz, D. Hariskos, E. Lotter, W. Witte, M. Powalla, Effects of heavy alkali elements in $Cu(In,Ga)Se_2$ solar cells with efficiencies up to 22.6%, Phys. Status Solidi RRL. 586 (2016) 583–586.

[2] http://www.solar-frontier.com/eng/news/2017/1220_press.html, 2017.

[3] White Paper for CIGS Thin Film Solar Cell Technology, 2016.
[4] P.C.K. Vesborg, T.F. Jaramillo, Addressing the terawatt challenge: scalability in the supply of chemical elements for renewable energy, R. Soc. Chem. Adv. 2 (2012) 7933-7947.
[5] C.S. Tao, J. Jiang, M. Tao, Natural resource limitations to terawatt-scale solar cells, Sol. Energy Mater. Sol. Cells. 95 (2011) 3176–3180.
[6] G. Yin, V. Brackmann, V. Hoffmann, M. Schmid, Enhanced performance of ultra-thin Cu(In,Ga)Se_2 solar cells deposited at low process temperature, Sol. Energy Mater. Sol. Cells. 132 (2015) 142–147.
[7] T. Nakada, Y. Hirabayashi, T. Tokado, D. Ohmori, T. Mise, Novel device structure for Cu(In,Ga)Se_2 thin film solar cells using transparent conducting oxide back and front contacts, Sol. Energy. 77 (2004) 739–747.
[8] M.D. Heinemann, V. Efimova, R. Klenk, B. Hoepfner, M. Wollgarten, T. Unold, H. Schock, C.A. Kaufmann, Cu(In,Ga)Se_2 superstrate solar cells : prospects and limitations, Prog. Photovolt: Res. Appl. 23 (2014) 1228-1237.
[9] G. Yin, M.W. Knight, M. Van Lare, M. Magdalena, S. Garcia, A. Polman, M. Schmid, Optoelectronic Enhancement of Ultrathin $CuIn_{1-x}Ga_xSe_2$ Solar Cells by Nanophotonic Contacts, Adv. Opt. Mater. 1600637 (2017).
[10] W.N. Shafarman, P.D. Paulson, Losses in $CuInSe_2$-based Thin Film Monolithic Tandem Solar Cells, Proc. 31th IEEE Photovoltaic Specialist Conf., IEEE, Lake Buena Vista, USA 2005
[11] M. Schmid, R. Caballero, R. Klenk, J. Krč, R. Klenk, T. Rissom, M. Topič, M.Ch. Lux-Steiner, Experimental verification of optically optimized $CuGaSe_2$ top cell for improving chalcopyrite tandems, PV Direct / EPJ Photovoltaics 1 (2010) 10601.
[12] P.J. Rostan, J. Mattheis, G. Bilger, U. Rau, J.H. Werner, Formation of transparent and ohmic ZnO:Al/$MoSe_2$ contacts for bifacial Cu(In,Ga)Se_2 solar cells and tandem structures, Thin Solid Films. 481 (2005) 67–70.
[13] J.K. Larsen, H. Simchi, P. Xin, K. Kim, W.N. Shafarman, Backwall superstrate configuration for ultrathin Cu(In,Ga)Se_2 solar cells, Appl. Phys. Lett. 033901 (2014).
[14] H. Simchi, J.K. Larsen, K. Kim, W.N. Shafarman, Improved Performance of Ultrathin Cu(In,Ga)Se_2 Solar Cells With a Backwall Superstrate Configuration, IEEE J. Photovolt. 4 (2014) 1630–1635.
[15] P.M.P. Salomé, B. Vermang, R. Ribeiro-andrade, J.P. Teixeira, J.M. V Cunha, M.J. Mendes, S. Haque, J. Borme, H. Águas, E. Fortunato, R. Martins, J.C. González, J.P. Leitão, P.A. Fernandes, M. Edoff, S. Sadewasser, Passivation of Interfaces in Thin Film Solar Cells : Understanding the Effects of a Nanostructured Rear Point Contact Layer, Adv. Mater. Interfaces.1701101 (2017) 1–10.
[16] N.A.R. Ezaei, O.L.I. Sabella, Z.E. V Roon, M. Zeman, Quenching Mo optical losses in CIGS solar cells by a point contacted dual-layer dielectric spacer : a 3-D optical study, Opt. Express. 26 (2018) 39–53.
[17] B. Vermang, J.T. Wätjen, V. Fjällström, F. Rostvall, M. Edoff, R. Kotipalli, F. Henry, D. Flandre, Employing Si solar cell technology to increase efficiency of ultra-thin Cu(In,Ga)Se_2 solar cells, Prog. Photovolt: Res. Appl. 22 (2014) 1023–1029.
[18] G. Yin, M. Song, S. Duan, P. Manley, D. Greiner, C.A. Kaufmann, M. Schmid,

Well-Controlled Dielectric Nanomeshes by Colloidal Nanosphere Lithography for Optoelectronic Enhancement of Ultrathin Cu(In,Ga)Se_2 Solar Cells, ACS Appl. Mater. Interfaces. 8 (2016) 31646–31652.
[19] S. Bose, J. M. V. Cunha, S. Suresh, J. D. Wild, T. S. Lopes, J. R. S. Barbosa, R. Silva, J. Borme, P. A. Fernandes, B. Vermang, P. M. P. Salome, Optical Lithography Patterning of SiO_2 Layers for Interface Passivation of Thin Film Solar Cells, Sol. RRL. 2(2018) 1800212.
[20] K. Chen, B.B. Rajeeva, Z. Wu, M. Rukavina, T.D. Dao, S. Ishii, M. Aono, T. Nagao, Y. Zheng, Moiré Nanosphere Lithography, ACS Nano 9 (2015) 6031–6040.
[21] P. Gao, J. He, S. Zhou, X. Yang, S. Li, J. Sheng, D. Wang, T. Yu, J. Ye, Y. Cui, Large-Area Nanosphere Self-Assembly by a Micro-Propulsive Injection Method for High Throughput Periodic Surface Nanotexturing, Nano Lett. 15 (2015) 4591–4598.
[22] A.M. Gabor, J.R. Tuttle, D.S. Albin, M.A. Contreras, R. Noufi, A.M. Hermann, High-efficiency Cu(In,Ga)Se_2 solar cells made from $(In,Ga)_2Se_3$ precursor films, Appl. Phys. Lett. 198 (2012) 3–6.
[23] A. Kosiorek, W. Kandulski, H. Glaczynska, M. Giersig, Fabrication of Nanoscale Rings , Dots , and Rods by Combining Shadow Nanosphere Lithography and Annealed Polystyrene Nanosphere Masks, Small. 1 (2005) 439–444.
[24] T. Sun, C.F. Guo, F. Cao, E.M. Akinoglu, Y. Wang, M. Giersig, Z. Ren, T. Sun, F. Guo, F. Cao, E.M. Akinoglu, Y. Wang, A broadband solar absorber with 12 nm thick ultrathin a-Si layer by using random metallic nanomeshes, Appl. Phys. Lett. 251119 (2015) 9–13.
[25] M. Schmid, Review on light management by nanostructures in chalcopyrite solar cells, Semicond. Sci. Technol. 32 (2017) 43003.
[26] G. Yin, C. Merschjann, M. Schmid, The effect of surface roughness on the determination of optical constants of $CuInSe_2$ and $CuGaSe_2$ thin films, J. Appl. Phys. 213510 (2013).
[27] G. Yin, P. Manley, M. Schmid, Influence of substrate and its temperature on the optical constants of Cu(In,Ga)Se_2 thin films, J. Phys. D: Appl. Phys. 47 (2014) 2–7.
[28] R. Kotipalli, O. Poncelet, G. Li, Y. Zeng, L.A. Francis, B. Vermang, D. Flandre, Addressing the impact of rear surface passivation mechanisms on ultra-thin Cu(In,Ga)Se_2 solar cell performances using SCAPS 1-D model, Sol. Energy. 157 (2017) 603–613.
[29] P. Casper, R Hunig, G. Gomard, O. Kiowski, C. Reitz, U. Lemmer, M. Powalla, M. Hetterich, Phys. Status Solidi RRL, 10 (2016) 376-380.
[30] H. Simchi, B.E. Mccandless, T. Meng, W.N. Shafarman, H. Simchi, B.E. Mccandless, T. Meng, W.N. Shafarman, Structure and interface chemistry of MoO_3 back contacts in Cu(In,Ga)Se_2 thin film solar cells, J. Appl. Phys. 033514 (2014).
[31] M. Burgelman, P. Nollet, S. Degrave, Modelling polycrystalline semiconductor solar cells, Thin Solid Films. 362 (2000) 527–532.
[32] B. Vermang, V. Fjällström, J. Pettersson, P. Salomé, M. Edoff, Development of rear surface passivated Cu(In,Ga)Se_2 thin film solar cells with nano-sized local rear point contacts, Sol. Energy Mater. Sol. Cells. 117 (2013) 505–511.
[33] G.T. Koishiyev, J.R. Sites, S.S. Kulkarni, N.G. Dhere, Determination of Back

Contact Barrier Height in Cu(In,Ga)(Se,S)$_2$ and CdTe Solar Celles, Proc. 33th IEEE Photovoltaic Specialist Conf., IEEE, Lake Buena Vista, USA, 2008.
[34] V.A. Online, K. Hsiao, H. Hsieh, T. Jiang, Electrical impact of $MoSe_2$ on CIGS thin-film solar cells, Phys. Chem. Chem. Phys. 15 (2013) 18174-18178.
[35] M. Moors, K. Baert, T. Caremans, F. Duerinckx, A. Cacciato, J. Szlufcik, Industrial PERL-type solar cells exceeding 19 % with screen-printed contacts and homogeneous emitter, Sol. Energy Mater. Sol. Cells. 106 (2012) 84–88.
[36] B. Vermang, H. Goverde, L. Tous, A. Lorenz, P. Choulat, J. Horzel, J. John, J. Poortmans, R. Mertens, Approach for Al_2O_3 rear surface passivation of industrial p-type Si PERC above 19%, Prog. Photovolt: Res. Appl. 20 (2012) 269–273.